Chemical Physics Letters 458 (2008) 134–137

Contents lists available at ScienceDirect

Chemical Physics Letters

journal homepage: www.elsevier.com/locate/cplett

Opto-electronic properties of titania nanotubes

M. Alam Khan [a,1], Hee-Tae Jung [b], O-Bong Yang [a,*]

[a] School of Semiconductor and Chemical Engineering, Chonbuk National University, Jeon-Ju 561-756, Republic of Korea
[b] Department of Chemical Biomolecular Engineering, Korea Advanced Institute of Science and Technology (KAIST), Dae-Jeon, Republic of Korea

ARTICLE INFO

Article history:
Received 2 January 2008
In final form 16 April 2008
Available online 22 April 2008

ABSTRACT

Opto-electronic properties of titanium oxide nanotubes (TiNT) were elucidated by photoluminescence (PL), UV-DRS and Raman spectroscopy. By hydrogen peroxide treatment of TiNTs, the PL intensity and selected area electron diffraction (SAED) patterns were notably increased, with the almost complete disappearance of the oxygen deficiency peaks in the Raman (279 cm^{-1}) and PL (391 and 409 nm) peaks, indicating improvements in the optical properties and crystallinity, as well as the recovery of oxygen vacancies to the stoichiometric titania.

1. Introduction

Titanium dioxide, a well-known oxide semiconductor material, has been extensively studied owing to its superior physical and chemical properties in photocatalysis [1,2]. Fine TiO_2 semiconductor nanoparticles are ideal photocatalytic materials due to their chemical stability, non-toxicity and high photocatalytic reactivity. It has been widely used in the elimination of pollutants [3], gas sensing [4], solar cells materials [5] and antifogging and self cleaning materials [6]. Fundamental physical properties of nanoscale materials are of interest, as the nano size and large surface area can lead to unexpected or dramatically unique properties [7]. The optical properties of anatase titania nanomaterials have been intensively studied since the opto-electronic properties of titania play a key role to determine their performance in optical sensors, photovoltaic cells and in photocatalytic reactions [8,9]. Most of attentions and efforts has been focused on the titania particles in terms of characterization of their crystallographic structures and microscopic morphologies but very little attention has been given to the electronic modification of 1D nanotubes. There are not much works on the titania nanotubes [10,11]. Furthermore, very little attention has been given to the electronic modification of titania nanotubes for its beneficial utilization. In our recent works on the titania nanotubes synthesized by hydrothermal method, we found the drastically increasing of its crystallinity by hydrogen peroxide treatment [11]. Herein, we elucidates the opto-electronic properties of titania nanotubes (TiNTs) by Raman, UV–Vis DRS and PL spectroscopy. It was found that hydrogen peroxide treatment of TiNT was essential for the enhancement of the optoelectronic properties of titania nanotubes, as indicated by the sharp, intense defects free PL and Raman spectras.

2. Experimental

For the synthesis of the titania nanotubes (TiNTs), the TiO_2 nanoparticles with the anatase phase only were prepared by mixing TiO_2/SiO_2 in mole ratio of 90:10 by addition of 52 mL titanium isopropoxide (TTIP, $Ti[OCH(CH_3)_2]_4$, >99%, Junsei Chemical Co.) and 5.2 mL of tetraethyl orthosilicate (TEOS, $Si(OC_2H_5)_4$, >99%, Acros Organics), dissolved in 52 mL of ethanol (99.5%). After refluxing this mixture solution at room temperature for 1 h, the second mixture of 52 mL of ethanol and 40.6 g of 4 M aqueous HCl (36%, Showa Chemical Co.) was added slowly to the first mixture solution and further stirred at room temperature for 1 h as described elsewhere [11], to form the precipitation of xerogel, the prepared sol was placed into the incubator at 80 °C for 48 h and then this xerogel was calcined in air at 600 °C for 3 h. The prepared and pulverized TiO_2 particles were treated by the hydrothermal method described by Kasuga et al. [12] except the hydrothermal temperature was maintained at 130 °C for 20 h in a Teflon lined high-pressure vessel, containing 100 ml of 8 M NaOH as an aqueous solution, with continuous stirring at 200 rpm. After aging and washing the precipitates, the powder was dried and calcined at 250 °C, which was denoted as TiNT-as prepared. TiNT-as prepared was treated with 2-wt% of aqueous hydrogen peroxide at 40 °C for 4 h, under mild reflux conditions in circular flask sealed and airtight in continuous inert (Ar) atmosphere. After the peroxide treatment the obtained sample posses yellow color. This sample was again washed with distilled water, vacuum filtered and calcined in air at 350 °C for 2 h. After calcination, it has white color and was denoted as TiNT–H_2O_2. All the titania nanotubes were calcined in air at 350 °C for 2 h before use and characterization. The crystal structures of samples were examined by high-resolution transmis-

* Corresponding author. Fax: +82 63 270 2306.
E-mail address: obyang@chonbuk.ac.kr (O-Bong Yang).
[1] Present address: School of Display and Chemical Engineering, Yeungnum University, 214-1 Dae-Dong, Gyeongsan 712-749, Republic of Korea.

0009-2614/$ - see front matter © 2008 Elsevier B.V. All rights reserved.
doi:10.1016/j.cplett.2008.04.073

sion electron microscopy (HR-TEM, Philips Technai 160 kV, three focused step, bright field). The TEM sample prepared by dispersing the TiNTs powder in alcohol by ultrasonic treatment applying a drop of the TiNTs to a carbon-coated copper grid. Particle sizes were determined from the micrographs recorded by Philips Technai 160 kV at transmission electron microscope. The opto-electronic properties of the TiNTs were explored using Raman (Raman microscope, Renishaw,s RenCam CCD detector with spectral resolution of 2 cm^{-1}), ultraviolet-visible diffuse reflectance spectra (UV–Vis DRS, Shimadzu UV 525) and Photoluminescence (PL, Flourospectroscopy 15 S).

3. Result and discussion

Fig. 1 shows the HR-TEM and selected area electron diffraction (SAED) images of the TiNT-as prepared and TiNT–H_2O_2. The detailed crystal structures of the TiNTs were shown to be well-defined, with both ended hollow nanotube growing along [001] directions with ~8 and ~5 nm outer and inner diameters, respectively. In the SAED images, the TiNT and TiNT–H_2O_2 were shown to be composed of anatase structural building units of the [101], [002] and [004] phases arising from the core of the nanotube. However, primary ([101] and [002]) and secondary ([004]) phase spots of TiNT–H_2O_2 were more prominent than those of TiNT-as prepared, where the spots were not distinct, indicating higher crystallinity of the former than of the latter. The chemical composition of the nanotubes was determined by energy dispersive X-ray with TEM (TEM-EDX, JEOL JEM–2010 high voltage range of 80–200 kV).The TiNTs were mainly composed of titanium, oxygen and sodium. A significant amount of sodium, 2.7%, was present as a counter cation in the TiNT-as prepared, but no sodium was detected in the TiNT–H_2O_2, which could be explained by that the substitution of the sodium cations by protons during the chemical treatment of the TiNT–H_2O_2. Average atomic ratios of oxygen to titanium were 1.78 and 1.97 in the TiNT-as prepared and TiNT–H_2O_2, respectively.

Fig. 2 shows the Raman spectra of the synthesized TiNTs and TiO_2 nanoparticles (Degussa, P25). It is well known that anatase phase has tetragonal (D_{4h}^{19}) phase, with six Raman active modes ($A_{1g} + 2B_{1g} + 3E_g$), while rutile tetragonal (D_{4h}^{14}) phase with four Raman active modes ($A_{1g} + B_{1g} + B_{2g} + E_g$) [13]. In the synthesized TiNT-as prepared, broad peaks at 197 (E_g), 279, 398 (B_{1g}), 442, 514 (A_{1g} and B_{1g}, unresolved), 642 cm^{-1} (E_g) and a shoulder at 702 cm^{-1} were observed. High intensity, broad peak between 240 and 290 cm^{-1} in titania nanocrystals are assigned to lattice-disorder or a second order effect resulted from defect-induced disorders [14,15]. This region of the spectrum, according to Barsani et al. [16,17] and Zhang et al. [18], was ascribe to oxygen deficiency and (or) the phonon confinement effects. So the strong and broad peak between 240 and 290 cm^{-1} (peaked at 279 cm^{-1}) in the TiNT-as prepared in our sample ascribe to be lattice-disorder or the oxygen deficiencies. In case of TiNT–H_2O_2, the Raman peaks were significantly increased after hydrogen peroxide treatment, except the two missing peaks at 279 cm^{-1} and 442 cm^{-1}, which are known as the peaks of oxygen vacancies and shoulder rutile phased, respectively [14,15]. This Raman result indicates that the hydrogen peroxide treatments of TiNTs is effective to the structural reformation towards perfect high crystalline anatase phase, with-

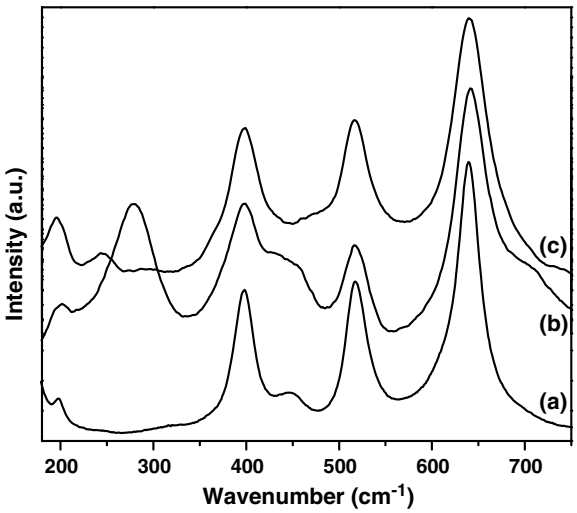

Fig. 2. Raman Spectra of (a) TiO_2 nanoparticle (P25), (b) TiNT-as prepared, and (c) TiNT–H_2O_2.

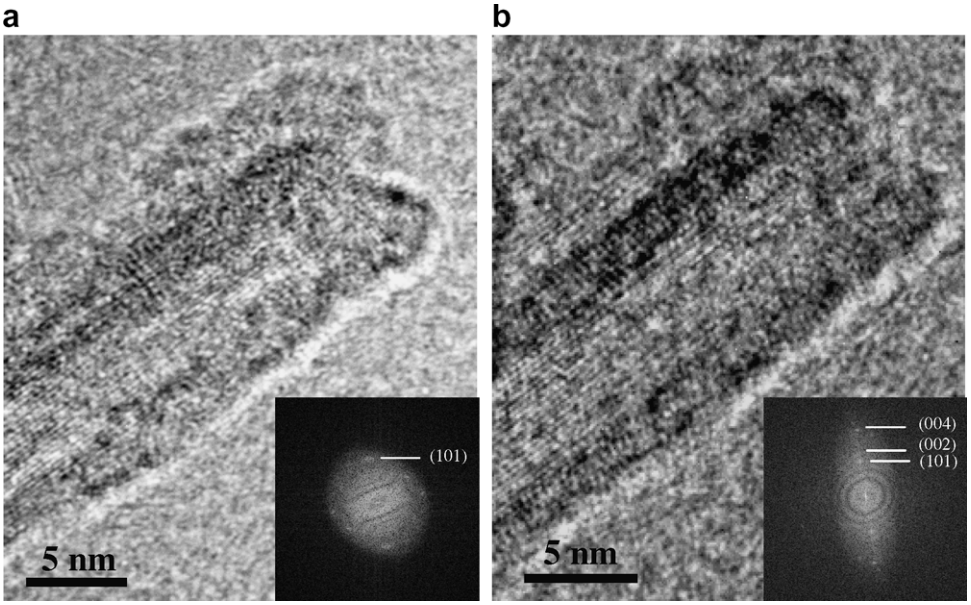

Fig. 1. (a) HR-TEM image of TiNT-as prepared and SAED pattern (inset). (b) HR-TEM image of TiNT–H_2O_2 and SAED pattern (inset).

out significant oxygen defects through cation exchange and the phase changed of some rutile shoulders to the anatase phase possibly arising due to experimental conditions. Only few oxygen vacancies still present in the TiNT–H_2O_2, as shown by the small oxygen vacancy peak at 244 cm^{-1} [12]. In terms of oxygen deficiency, this Raman result was consistent with the TEM-EDX result which shows almost stoichiometric atomic ratios, 1.97 of oxygen to titanium. The Raman spectra of TiNTs are significantly different from those of sodium titanates, $Na_2Ti_3O_7/H_2Ti_3O_7$ and $Na_2Ti_3O_7/H_2Ti_3O_7$, which show sharp peaks at wave numbers lower than 400 cm^{-1} [19]. Moreover, Raman active peaks due to impurities and reaction products were not observed in any of the TiNTs, indicating that TiNT–H_2O_2 has a uniform morphology, with a good quality pure anatase phase. Although the size and morphology difference, there are no significant difference in Raman shift between nanotubes and nanoparticle [20] of titania.

The possibility of peroxo group effect on nanotubes was observed by UV–Vis DRS results shown in Fig. 3, where absorption peaks of TiO_2 nanoparticles (Degussa P25), TiNT-as prepared and TiNT–H_2O_2 were very similar to each other, resulting from the maintenance of crystal octahedra and framework of titania having similar band gap energies. This indicates that band structure of TiNT-as prepared have little shallow bending to that TiO_2 nanoparticles (Degussa P25), and TiNT–H_2O_2 possibly due the oxygen vacancies in the crystal framework. Thus UV–Vis absorption spectra are agreed with visual observations of TiNT-as prepared and TiNT–H_2O_2, where peroxo group vanishes after calcinations.

Photoluminescence (PL) is an extremely useful tool for obtaining information about the electronic, optic and photoelectric properties of materials. PL spectra are closely related to the surface stoichiometry and surface states of nanomaterials [21]. It is well known that PL spectra are affected greatly as a function of particle size [21].

The higher the intensity of the peaks in PL spectra the more uniform interfaces with no trap sites on their surfaces [19,21]. No detailed analysis of PL spectra for titania nanotube has ever been conducted, although there are many reports on TiO_2 nanoparticles. To examine the photoelectronic properties of the titania nanotubes, PL spectra, excited at 310 nm and room temperature, were measured for TiNT-as prepared, TiNT–H_2O_2 and TiO_2 nanoparticles (Degussa P25), as shown in Fig. 4. The PL spectrum was deconvoluted by multiple Gaussian fitting. The intensity of the TiNT–H_2O_2 spectrum significantly increased ca. 2 and 3 times, compared

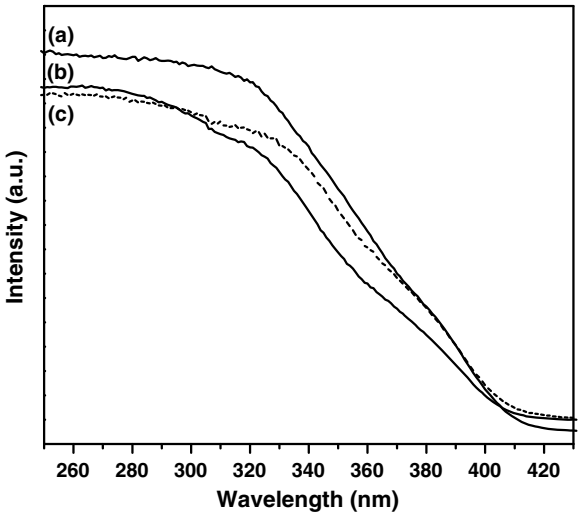

Fig. 3. UV–Vis DRS Spectra of (a) TiO_2 nanoparticle (P25), (b) TiNT-as prepared, and (c) TiNT–H_2O_2.

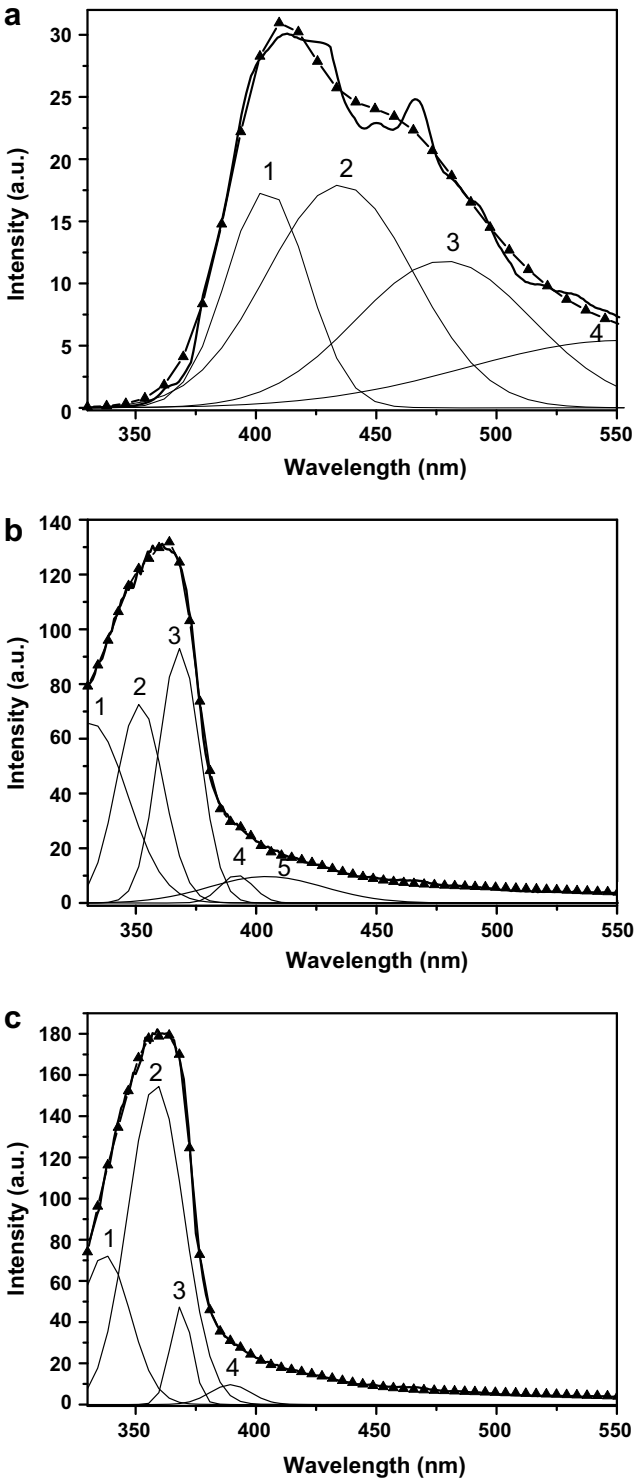

Fig. 4. PL spectra of (a) TiO_2 nanoparticles (P25), (b) TiNT-as prepared, and (c) TiNT–H_2O_2. The filled triangle is the summation of all the deconvoluted peaks.

to those for TiNT-as prepared and TiO_2 (P25) nanoparticles, respectively, indicating enhancement of the optical properties due to hydrogen peroxide treatment. The main spectral bands of TiNT–H_2O_2, TiNT-as prepared and TiO_2 (P25) nanoparticles peaked at 357, 363 and 412 nm, respectively. The broadening of the peak in TiNT-as prepared may be due to the surface roughness and defects, which may break the periodicity of lattices. Consequently, PL spectrum shifts to the lower energy region and becomes broader.

However, these defects and perturbations were substantially removed by the hydrogen peroxide treatment. It is interesting that the PL spectra of TiNTs are shifted towards the blue region of the spectrum, ca. 50 nm, compared to that for TiO_2 (Degussa P25) nanoparticles. This blue shift may be attributed to the reduction of size and grain boundaries, from 25 nm of TiO_2 particles to ca. ~8 nm (diameter) of TiNTs. This result suggests the surface states such as impurities and oxidation states of the octahedra, bond angles and bond lengths are rearranged during the formation of nanotubes in the hydrothermal process. The presences of rutile phases in the nanocrystals are known to cause a significant decrease in the PL intensity [21]. The high intensity of the PL spectrum for TiNT–H_2O_2 compared to TiNT-as prepared seems to be due to the superior optical properties, as well as the absence of the small rutile shoulder, as shown in Raman spectra.

The PL spectrum of anatase phase titania resulted from three origins: self trapped excitons [22,24], surface states [23] and oxygen vacancies [22,24]. The broad PL spectrum of TiO_2 nanoparticles (Degussa P25) was deconvoluted by four Gaussian peaks: (i) oxygen octahedral peaks at 412 (peak 1) and 434 nm (peak 2); and (ii) rutile peak at 478 (peak 3) and oxygen vacancy peak at longer wavelength region of 543 nm (peak 4) [22]. This broad PL spectrum may be ascribed to the rutile phases and heterogeneous surface properties, which is consistent with our data's. Despite the substantial peak shift in the TiNTs spectra, the PL spectrum of TiNT-as prepared can be assigned as consisting of two kinds of peak; (i) oxygen octahedral peaks at 334 (peak 1), 351 (peak 2) and 368 nm (peak 3); and (ii) oxygen vacancy peaks at 391 (peak 4) and 409 nm (peak 5). The positions and shapes of the Gaussian peak of TiO_6 octahedra in TiNTs were almost identical. The absence of the oxygen vacancy peak at 409 nm (peak 5) in the spectrum for TiNT–H_2O_2 indicates recovery of the oxygen vacancies due to hydrogen peroxide treatment, which was consistent with the EDX and Raman spectra. For the formation of nanotube by the hydrothermal method, it has been conjectured that the resulting crystalline surface is corrupted, and Ti–O–Ti linkages of TiO_2 octahedra are broken under the strong alkali solutions, leaving some oxygen vacancies in TiNT-as prepared. In the case of oxygen vacancies, it is still not clear which kinds of vacancies are prevailing. However, it is speculated that edge sharing oxygen atoms are more prone to the oxygen vacancies which were almost recovered and balanced due to the chemisorption to a stoichiometric ratio of titanium dioxide after hydrogen peroxide treatment. And further calcination at 350 °C make the strong titania octahedra. These finding were consistent with Raman spectra where the reduced oxygen vacancy peak at 240 and 290 cm^{-1} were observed. PL spectra depend strongly on particle sizes, defects and impurities, which may be due to the rearrangement of the bond angles and length at the surfaces. The formation of nanotube may lead to a drastic peak shift and band narrowing, resulting in optimized localized states of TiNTs [21]. The higher and sharper the PL intensity, the more uniform surface states of the titanium in TiNT–H_2O_2. The more prominent blue shift in TiNT–H_2O_2 compared to TiNT-as prepared may be due to the recovery of oxygen defects and the removal of surface impurities, such as sodium.

4. Conclusion

In conclusion, optoelectronic properties of titania nanotubes were elucidated by Raman, PL and UV–DRS spectra. After the hydrogen peroxide treatment of TiNTs, optical properties of PL peak intensity and sharpness were significantly increased owing to the recovery of oxygen vacancies. The PL spectra for TiNTs (diameter ca. 8 nm) were significantly shifted toward the blue region (ca. 50 nm) compared to TiO_2 nanoparticles (size ca. 25 nm) due to the nano size effect. Band gap energy was not much affected showing intact TiO_6 octahedra. Optoelectronic properties of TiNTs were strongly affected by the hydrogen peroxide treatment. Raman, PL and UV–DRS spectra were useful tools for characterizing details of opto-electronic properties of titania nanotubes and nanoparticles.

Acknowledgements

We gratefully acknowledge the financial support from the Korea Industry Technology Foundation, by the program of the Human Resources Development for Regional Innovation and the Center for Ultra micro chemical Process Systems (CUPS), sponsored by the Korea Science and Engineering Foundation (KOSEF). M.A. Khan would like to thank BK21 program for the financial support.

References

[1] A. Fujishima, K. Honda, Nature 238 (1972) 37.
[2] A.L. Linsebigler, G. Lu, J.T. Yates, Chem. Rev. 95 (1995) 735.
[3] A. Fujishima, T.N. Rao, D.A. Tryk, J. Photochem. Photobiol. 1 (2000) 1.
[4] L.R. Skubal, N.K. Meshkov, M.C. Vogt, J. Photochem. Photobiol. A 148 (2002) 103.
[5] O'B. Regan, M. Grätzel, Nature 353 (1991) 737.
[6] R. Wang, K. Hashimoto, A. Fujishima, Nature 338 (1997) 431.
[7] R.D. Andres et al., J. Mater. Res. 4 (1989) 704.
[8] M.E. Davis, Nature 417 (2002) 813.
[9] S. Inagaki, S. Guan, T. Ohsuna, O. Terasaki, Nature 416 (2002) 304.
[10] K. Zhu, N.R. Neale, A. Miedaner, Arthur J. Frank, Nano Lett. 7 (2007) 69.
[11] M.A. Khan, H.-T. Jung, O-Bong Yang, J. Phys. Chem. B 110 (2006) 6626.
[12] T. Kasuga, M. Hiramatsu, A. Honson, T. Sekino, T. Niihara, Langmuir 14 (1998) 160.
[13] P.P. Lottici, D. Barsani, M. Braghini, A. Montenero, J. Mater. Sci. 28 (1993) 177.
[14] T. Oshaka, J. Phys. Soc. Jpn. 1661 (1980) 48.
[15] R.J. Betsch, H.L. Park, W.B. White, Mater. Res. Bull. 26 (1991) 613.
[16] D. Bersani, G. Antonioli, P.P. Lottici, T. Lopez, J. Non-Cryst. Solids 175 (1998) 232.
[17] D. Bersani, P.P. Lottici, T. Lopez, X.Z. Ding, J. Sol–gel Sci. Technol. 13 (1998) 849.
[18] W.F. Zhang, Y.L. He, M.S. Zhang, Z. Yin, Q. Chen, J. Phys. D: Appl. Phys. 33 (2000) 912.
[19] C.E. Bamberger, G. Begum, J. Am. Ceram. Soc. 70 (1987) 48.
[20] D. Bersani, P.P. Lottici, Appl. Phys. Lett. 72 (1998) 73.
[21] W.F. Zhang, M.S. Zhang, Z. Yin, Phys. Stat. Sol. 179 (2000) 319.
[22] L.V. Saraf, S.I. Patil, S.B. Ogale, S.R. Sainkar, S.T. Kshirsager, Int. J. Mod. Phys. B12 (1998) 2635.
[23] L. Fross, M. Schubnell, Appl. Phys. B: Photophys. Laser Chem. 56 (1993) 363.
[24] H. Tang, H. Berger, P.E. Schmid, F. Levy, Solid State Commun. 87 (1993) 847.